J Mater Sci (2008) 43:2713–2720
DOI 10.1007/s10853-008-2485-5

Cation dopant effect on phase transformation and microstructural evolution in M^{2+}-substituted γ-alumina powders

**Atsushi Odaka · Tomohiro Yamaguchi ·
Takayuki Fujita · Seiichi Taruta · Kunio Kitajima**

Received: 19 October 2007 / Accepted: 18 January 2008 / Published online: 21 February 2008

Abstract The effect of divalent cation dopants on the phase transformation and microstructural evolution in M^{2+}-substituted γ-alumina (GA-M; M = Mg, Ca, Sr, Mn, Co, Ni, Cu, Zn; 0.1–0.5 mol%) powders were systematically investigated. Divalent cations were substituted into the defect spinel lattice of γ-alumina through a sol–gel route using high-purity polyhydroxoaluminum and MCl_2 solutions. All divalent dopants retarded γ-to-α transformation up to 0.3 mol%. A correlation was found between the transformation temperature and the ionic radius of dopant at 0.5 mol% with the exception of the Cu series, where eutectic liquid formation may occur. The microstructural evolution in GA-M powders at high temperature was strongly affected by dopants that segregated from GA-M primary particles to the grain boundary during/after transformation. All dopant effects on grain growth in GA-M powders at 0.1 mol% were retarding. Average grain size at high temperatures seemed to correlate with dopant ionic radius, excepting Cu and Mn.

Introduction

The microstructure must be carefully controlled to obtain dense and fine-grained alumina ceramics with improved properties. In order to obtain fine-grained or nanocrystalline alumina ceramics, some studies focused on the use of nanosized transition alumina powders [1, 2]. In these studies, alumina ceramics with a grain size of 200 nm or less were obtained by pressure sintering. We focused on the use of polyhydroxoaluminum (PHA) gel-derived transition alumina powders [3–6]. Fully densified alumina ceramics were obtained by pulse electric current sintering [5], and a fine-grained microstructure with an average size of 0.47 μm would be obtained [6].

Dopant or co-dopant additives such as MgO, CaO, and NiO are known to influence the sintering and grain growth of α-alumina [7–12]. Dopants tend to segregate to grain boundaries or form second-phase precipitates [13], acting as solute drag to reduce the grain boundary mobility [8, 9]. There are, however, a few reports concerning the effects of additives on sintering behavior of transition alumina powders: for θ-alumina [14], in which MgO is incorporated by the solution impregnation method, and for Mg^{2+}-doped γ-alumina [6] obtained from PHA solution by a sol–gel process. However, the effect of various cation additives on the phase transformation of γ-alumina powder was studied extensively using impregnated γ-alumina powder with a high loading of such as 10 mol% [15–18]. The phase transformation of transition aluminas is also important for the sintering and control of microstructure in alumina ceramics.

If various divalent cation-substituted γ-alumina powders, in which divalent cations are directly substituted into the defect spinel lattice of γ-alumina [6], can be obtained, this can potentially extend the use of substituted powders to the fabrication of fine-grained ceramics by selecting appropriate dopants. Thus, in the course of developing nanosized alumina starting powders, the present work deals with the formation of divalent M^{2+} cation substituted

---

A. Odaka · T. Yamaguchi (✉) · S. Taruta · K. Kitajima
Department of Chemistry and Material Engineering,
Faculty of Engineering, Shinshu University,
4-17-1 Wakasato, Nagano-shi 380-8553, Japan
e-mail: mtmouth@shinshu-u.ac.jp

T. Fujita
Taimei Chemicals Co. Ltd, 4150 Minamiminowa-mura,
Kamiina-gun, Nagano 399-4597, Japan

γ-alumina (GA-M, M = Mg, Ca, Sr, Mn, Co, Ni, Cu, and Zn; 0.1–0.5 mol%) powders. The aim of the present study is to determine substitutional M^{2+}-dopant effects on the phase transformation and high-temperature microstructural evolution in GA-M powders for a better understanding of the thermal behavior of GA-M powders. The GA-M powders were prepared by a new sol–gel route using high-purity PHA and MCl_2 solutions as starting materials. The substitutional dopant effect in GA-M powders, along with their nanosized nature, would demonstrate the higher effect of dispersed dopants on microstructural evolution, compared with that in α-alumina or transition alumina powders doped by the impregnation method.

Experimental

A high-purity PHA solution having an Al_2O_3 concentration of 23.7 mass% and a OH/Al ratio of 2.50 was prepared by dissolving Al metal in HCl solution [19]. Special attention was paid to impurities. The sources of divalent cations were $MCl_2 \cdot nH_2O$ (M = Mg, Ca, Sr, Mn, Co, Ni, Cu, and Zn, $n = 2$, 4 or 6, Wako Pure Chemical Industries, Japan). Each chloride was dissolved in distilled water and added to the PHA solution to form 0, 0.10, 0.30, 0.50, and 2.00 mol% M^{2+} against the mole of Al_2O_3 obtained from the PHA solution. The mixed solutions were stirred thoroughly at room temperature and then held at 60 °C for 2 days or more for gelation. The resultant gels were ground into –150 μm powders using a high-purity alumina mortar and pestle and then calcined at 900 °C for 3 h to obtain GA-M (hereafter abbreviated, for example, as GA-M0.5 and GA-M2 for 0.50 and 2.00 mol% dopant, respectively) powders. The GA-M powders were pulverized again and sieved through a 140-mesh (–106 μm) screen. The amounts of impurities (by mass), as measured by ICP after dissolution, in GA-Ni0.5, for example, were 21 ppm Si, 14 ppm Na, 3 ppm Ca, and 30 ppm Fe, showing that the purity was higher than 99.99%. In order to determine the phase transformation temperature, DTA (TG 8120, Rigaku, Japan) measurements were conducted at a heating rate of 10 °C/min under flowing air using 25 mg samples. The GA-M powders were heated at 1,050–1,400°C for 3 h. Their phases were characterized by powder XRD, using monochromatic CuKα radiation (RINT 2000, Rigaku). The microstructure of the GA-M powders was observed by a scanning electron microscope (S-3100H, Hitachi, Japan) and a transmission electron microscope (JEM-2010, JEOL, Japan). TEM samples were prepared by suspending the lightly ground GA-M powders in ethanol and evaporating a droplet of the suspension onto a microgrid. The average grain size of the sintered powders was estimated by the line–intercept method with paying very careful attention to defining the grain boundary positions, using the magnified SEM and TEM photographs and part of the results obtained from SEM were compared with those obtained from TEM to ascertain the accuracy of grain size measurements. The average grain size was determined by using at least 100 grain size measurements.

Results and discussion

Phase transformation in M^{2+}-substituted γ-alumina powders

Figure 1 shows the XRD patterns of typical GA-M0.5 powders obtained from the corresponding starting gels. While the undoped GA-M0 powder consisted of γ-alumina with a trace of χ-alumina, the characteristic diffraction of χ-alumina at around 42.5° [20, 21] was absent in all GA-M0.5 samples. This implies that a small amount of divalent dopant is sufficient to suppress the co-formation of χ-alumina. Moreover, the diffraction peak around 67° shifted to lower diffraction angles with increasing dopant content. Indeed, the GA-Ni sample containing 20 mol% Ni^{2+}, for example, yielded a single-phase γ-alumina with a larger lattice constant ($a_0 = 0.797$ nm) than that of GA-M0 ($a_0 = 0.788$ nm). This indicates that the solid solutions containing Ni^{2+} cations in the defect spinel lattice of γ-alumina were formed between 0 and 20 mol%, as in the case of Mg^{2+} reported previously [6]. These chemical lattice

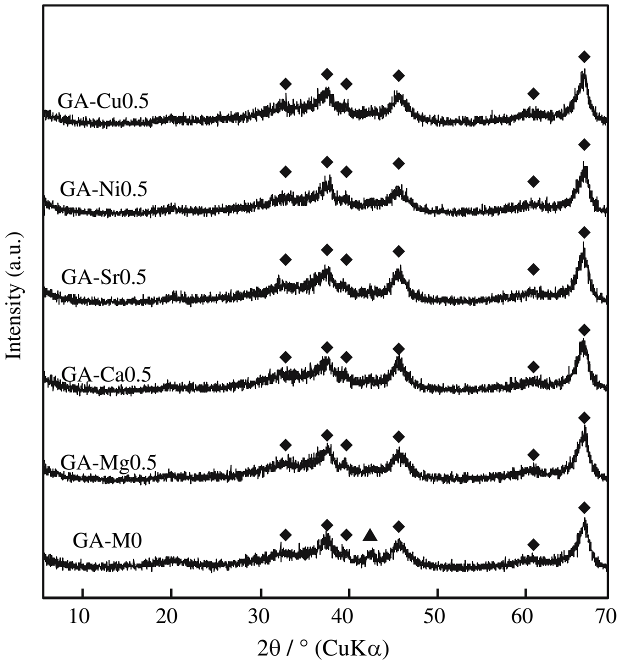

Fig. 1 XRD patterns of various GA-M powders. ◆: γ-Al_2O_3, ▲: χ-Al_2O_3

expansions were also observed for other GA-M samples having higher M^{2+} substitutions, except the Ca and Sr series.

For the Ca and Sr series, increase in the lattice constant was saturated around 0.5 mol%. This indicates that the solubility of Ca^{2+} and Sr^{2+} in the γ-alumina lattice is very low owing to their larger cation sizes, but that the dopant cations were substituted even for the Ca and Sr series at least up to around 0.5 mol%.

Figure 2 shows the DTA curves of GA-Ca and GA-Cu series powders with increasing dopant content, along with that of GA-M0 as a reference. The exothermic peak, which was attributed to the γ-to-α transformation [3] by XRD, was located at 1,151 °C for GA-M0. The exothermic peak for the GA-Ca series shifted to higher temperatures and weakened with increasing substitution. In contrast, the exothermic peak for the GA-Cu series shifted to higher temperatures up to 0.3 mol% and then to lower temperatures above 0.3 mol% with a marked sharpening at 2 mol%. This suggests that the transformation mechanism changed around 0.3 mol%.

Figure 3 plots the exothermic peak temperature (T_p) against the Ca-, Ni-, and Cu-dopant content. Clearly, the transformation temperature strongly depended on the dopant content. The T_p of the GA-Ca series increased markedly up to 1.25 mol% and gradually above 1.25 mol%, while that of the GA-Cu series increased up to 0.3 mol% but decreased above 0.3 mol%. The T_p of the GA-Ni series increased monotonically up to 2 mol%. These results show that only a small amount of dopant is enough for systematic changes in the transformation behavior of GA-M powders. This is an important feature of the present GA-M series powders, as distinct from the impregnated γ-alumina powders. For example, the increase in the transformation temperature of the Ni-impregnated sample (10 mol%) was 4 K [15], while that for the GA-Ni0.5 powder was 10 K. The effect of substitutional dopants (0.5 mol%) was clear. Thus, the present study focused on the dopant effect on transformation in the GA-M0.5 series.

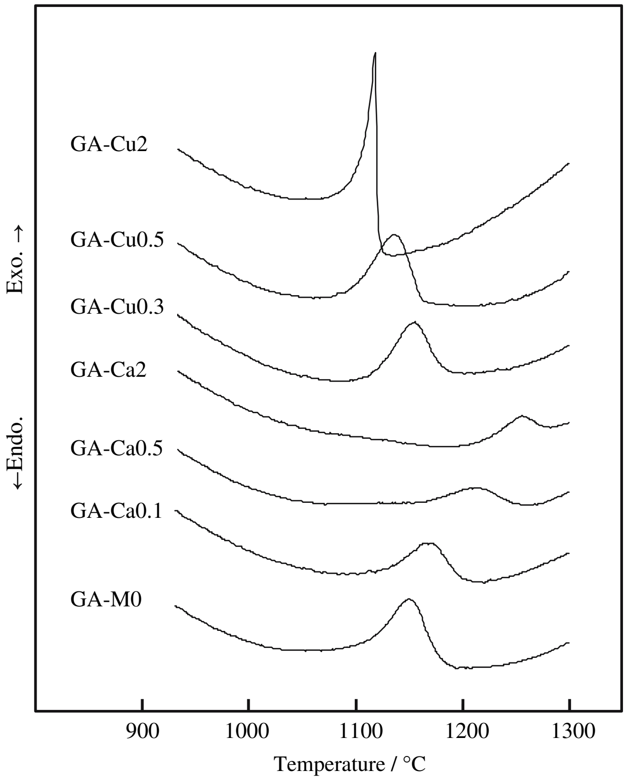

Fig. 2 DTA curves of GA-Ca and GA-Cu powders having different dopant contents

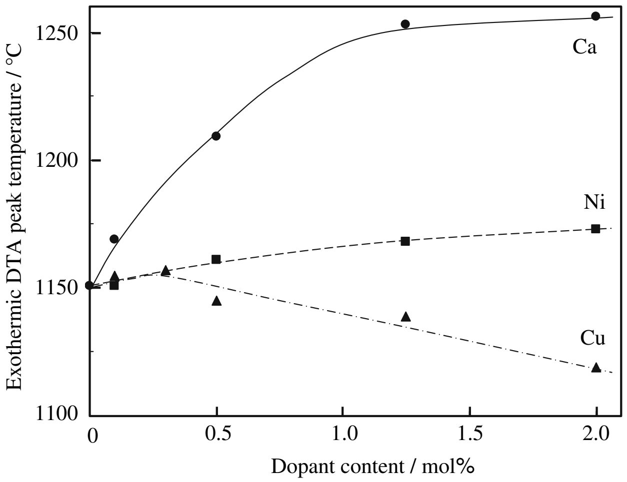

Fig. 3 Exothermic DTA peak temperature plotted against cation dopant content for GA-Ca, GA-Cu, and GA-Ni powders. ●: Ca, ▲: Cu, ■: Ni

Figure 4 shows the DTA curves of typical GA-M05 powders. The transformation is clearly very sensitive to the

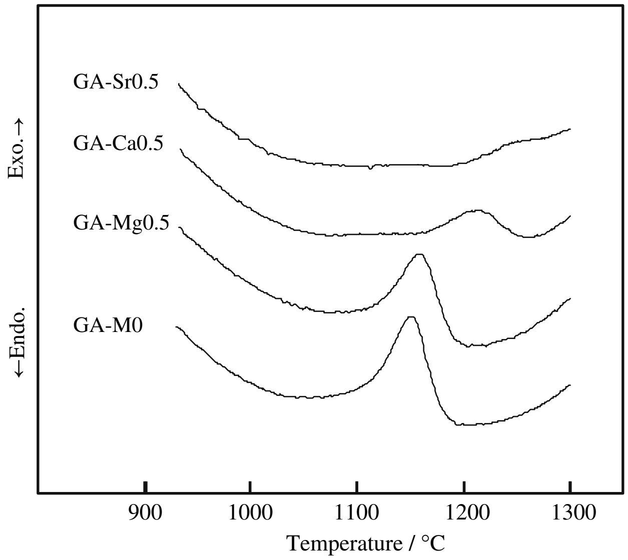

Fig. 4 DTA curves of GA-M0.5 powders having different cation dopants

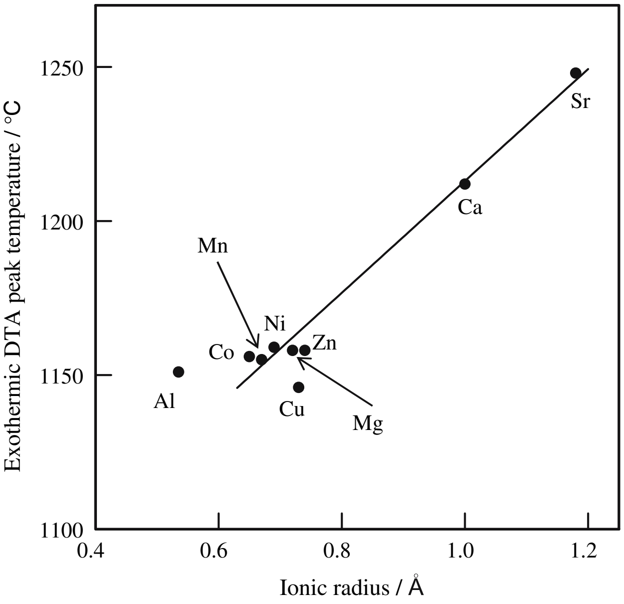

Fig. 5 Exothermic DTA peak temperature plotted against the ionic radius of divalent cation dopant for various GA-M0.5 powders.

dopant species. In particular, in the case of alkaline earth series dopants, the ionic radius of the dopant seems to play an important role in the shift of the exothermic peak, i.e., the phase transformation, as observed for impregnated powders by Okada et al. [15]. Thus, Figure 5 plots the T_p of GA-M0.5 powders against the ionic radius for sixfold coordination [15, 22] of dopants. It is seen that the dopants fall into one of these three groups: those having (i) a weak retarding effect (Mg, Mn, Co, Ni, and Zn), (ii) a strong retarding effect (Ca, Sr), and (iii) a weak accelerating effect (Cu). Overall, the dopant effects in GA-M powders are analogous to those in impregnated γ-alumina powders [15], however, some differences are observed: the addition of CuO and MnO (10 mol%) by impregnation caused a dramatic decrease in T_p. Moreover, it should be noted that all divalent dopants studied here retarded the transformation up to 0.3 mol%, where the Cu dopant was reclassified into group (i). This indicates that M^{2+}-dopants should thermodynamically decrease the free energy (G) of γ-alumina relative to that of corundum, causing the phase transformation temperature to shift up. The difference in the effect of Cu and Mn dopants between the present system and that studied by Okada et al. [15] can be attributed to the difference in the dopant content and doping conditions, whether or not the dopants are substituted directly into the lattice in the starting powders. The T_p lowering in GA-Cu powders above 0.3 mol% can be explained by the eutectic liquid formation of Al_2O_3–CuO–Cu_2O, which accelerates the transformation [15]. This is supported by the fact that the DTA baseline of GA-Cu2 showed a remarkable shift towards the endothermic side, exhibiting a change in curvature around 1,120–1,160°C (Fig. 2).

T_p appears to correlate with the dopant ionic radius: the transformation tends to be retarded with increasing substitutional dopant radius. The thermal stability of the substituted γ-alumina lattice is enhanced by larger substitutional dopants, especially in the case of alkaline earth dopants. A substitutional dopant with larger ionic radius is thought to be more effective in suppressing the diffusion of Al^{3+} and O^{2-} in the lattice [15], and hence retards the transformation by suppressing the rearrangement of oxygen anions from fcc to hcp packing [23]. This tendency to enhance thermal stability is analogous to that reported for impregnated powders [15]. Site preference of dopants to tetrahedral or octahedral sites in the γ-alumina lattice might also modulate the degree of retardation. However, further discussion is difficult because dopant sites are unknown in the present samples.

Clearly, the phase transformation in GA-M powders is more strongly affected by even a small amount of dopant owing to the intimate mixing at the atomic level, compared with that in impregnated powders. The phase transformation in GA-M powders is affected directly by substitutional dopants in the lattice, while that in impregnated powders is indirectly affected by the interaction between γ-alumina particles and the impregnated dopants upon heating. It has been reported [15] that some dopants in impregnated powders became incorporated into the γ-alumina lattice during the heating process, however, the GA-M powders prepared by the sol–gel method in the present study are attractive from the standpoint of reducing the dopant content to fabricate fine-grained alumina ceramics by minimizing the precipitation of the secondary phase. In fact, the second phase could not be detected by XRD using high powered X-rays in GA-M0.1 samples after firing at 1,200–1,400 °C. In the case of GA-M0.5 powders, the excess segregated dopants precipitated in small quantities as a second phase, such as $MAl_{12}O_{19}$ [magnetoplumbite-type] for Ca and Sr, and MAl_2O_4 [spinel-type] for the other dopants above 1,200 °C. The critical concentration for secondary phase formation depended on the dopant content and the grain size developed [24].

Microstructural evolution in M^{2+}-substituted γ-alumina powders

In order to investigate the dopant effect on microstructural evolution under little or no secondary phase precipitation, our study focused mainly on GA-M0.1 powders. Figure 6 shows TEM images of GA-M0 and GA-Ca0.1 samples heated at 1,050 °C for 3 h. GA-M0 yielded two types of particles having different morphologies: large grains

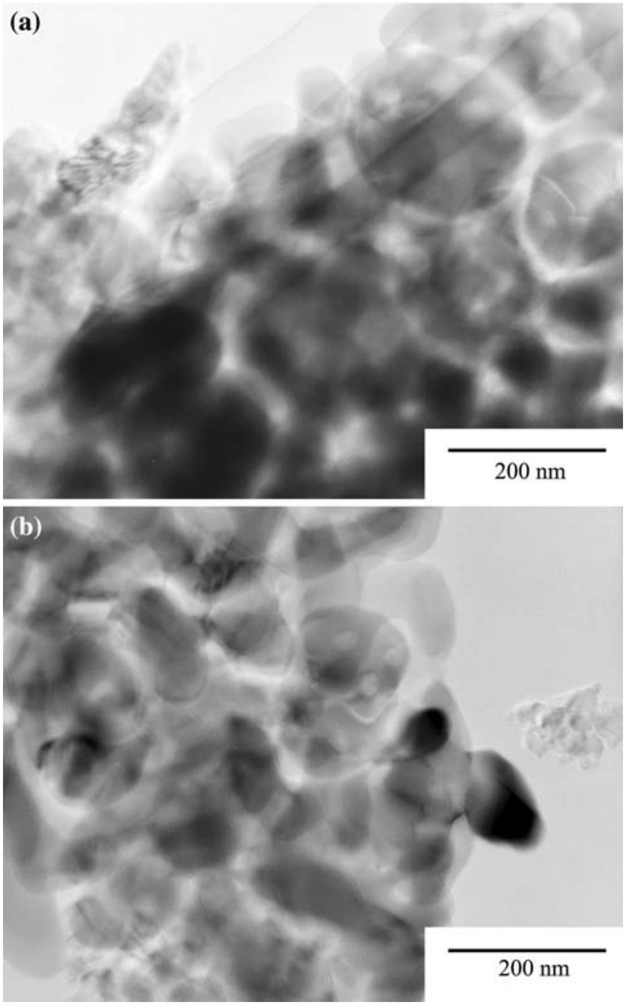

Fig. 6 TEM photographs of (**a**) GA-M0 and (**b**) GA-Ca0.1 samples heated at 1,050 °C

(around 140 nm) of α-alumina and aggregates of smaller particles (around 15 nm) of γ-alumina. GA-Ca0.1 also yielded two types of particles, however, the α-alumina grains were smaller (around 100 nm). These results indicate that α-alumina grew rapidly and that the dopant Ca significantly suppressed the grain growth of α-alumina in the primary particle matrices during sintering.

The retardation in transformation was favorable for the evolution of a fine-grained microstructure. However, the retardation of grain growth in GA-Ca0.1 samples was mainly attributable to the Ca doping, rather than the increased transformation temperature, because the difference (ΔT) in T_p between the GA-M0 and GA-Ca0.1 samples was very small (18 K). In general, the mechanism for α-transformation consists of nucleation and growth [25], and many researchers have reported the rapid growth of α-alumina [21, 25, 26].

Figure 7 shows the microstructure of typical GA-M0.1 samples (M = Ca, Ni, and Cu) sintered at 1,200 °C along with the undoped sample GA-M0. The undoped sample evolved a ‘vermicular’ microstructure [25, 27] that contained continuous grains of α-alumina (around 0.25 μm) and pore channels. GA-M0.1 powders also exhibited a vermicular microstructure, however, their grain sizes strongly depended on the dopant species: even a small amount of dopant affected the microstructural evolution. The Ca dopant resulted in a marked decrease in grain size, while Ni caused a slight decrease. The Cu dopant caused little change in grain growth at 0.1 mol%. Although grain growth in GA-M powders resulted in a vermicular microstructure, the grains grew along contiguous paths of connectivity (grain boundaries). Thus, the microstructure of GA-M0.1 was possibly determined by highly dispersed dopants expelled from GA-M primary particles and segregating at the grain boundary and grain surfaces during the grain growth that occurred with/after the transformation.

Figure 8 shows the microstructure of typical GA-M0.1 samples (M = Ca, Ni, and Cu) that evolved at 1,400 °C. The grain growth behaviors were more pronounced at higher temperatures. The GA-M0 sample retained a vermicular microstructure at an increased average grain size of about 0.57 μm. Grain growth in the GA-Ca0.1 was markedly suppressed, while that in GA-Cu0.1 powder was only slightly suppressed. Grain growth in GA-Ni0.1 was also suppressed. Thus, substitutional M^{2+}-dopants in the γ-alumina lattice resulted in the development of a uniform microstructure with a narrow grain size distribution upon heating.

For systematic representation, Fig. 9 plots the average grain size of GA-M0.1 samples prepared at 1,200 °C against the ionic radius of dopant, along with that developed at 1,400 °C. The average grain size was measured by SEM. The data shown in Fig. 9 are in good agreement with those of the TEM observation within 5% deviation. The cation dopant effect for GA-M0.1 samples at 1,200 °C was all retarding, falling into one of the three categories: (i) weak retarding effect for Cu, (ii) moderate retarding effect for Mg, Mn, Co, Ni, and Zn, and (iii) a strong retarding effect for Ca and Sr. The cation dopant effect for GA-M0.1 samples at 1,400 °C was also all retarding, similarly to that at 1,200 °C. The Mn series changed its degree of retarding effect at 1,400 °C and fell into group (i). The retarding effect of Mg and Ni dopant was similar to those reported for MgO and NiO added θ-alumina powder [14]. The suppression effect on grain growth, especially in GA-M0.1 samples, seemed to correlate with the ionic radius of dopant: the grain size of GA-M0.1 samples tended to decrease as the ionic radius of dopant increased. This trend, when compared with Fig. 5, can be interpreted as suggesting that the retardation of grain growth correlates with the retardation in transformation. However, ΔT in the T_p among the GA-M0.1 series was very small, minimizing the

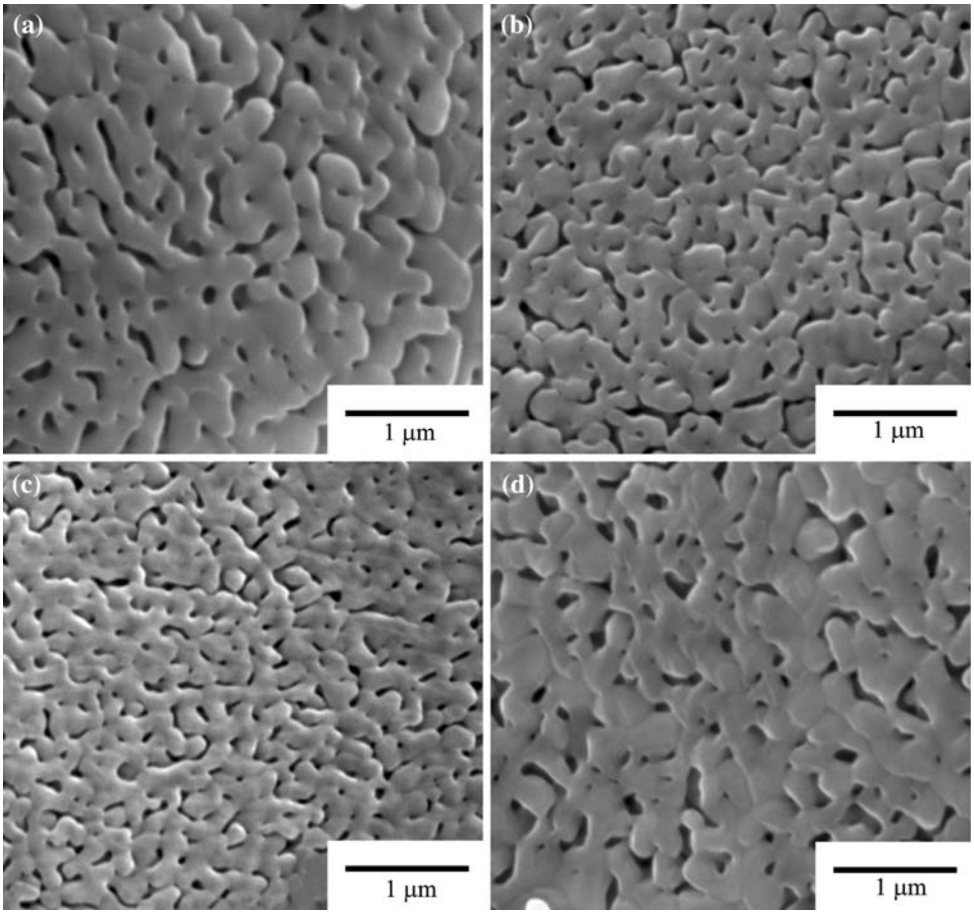

Fig. 7 SEM photographs of typical GA-M01 samples sintered at 1,200 °C for 3 h. (**a**) GA-M0, (**b**) GA-Ni0.1, (**c**) GA-Ca0.1, and (**d**) GA-Cu0.1

effect of ΔT on grain growth under prolonged heating conditions, e.g., 3 h. Thus, it is reasonable to conclude that the grain size developed was predominantly affected by the segregated dopants themselves, suggesting that the dopant affects both the grain growth and transformation retardation through a similar mechanism.

Recently, the segregated dopant effect (0.1 mol%, Mg, Mn, Sr, etc.) on the grain boundary diffusivity in alumina was shown to relate to the ionicity in the vicinity of the grain boundaries: the improved ionicity presumably suppresses the atomic diffusion through the increase in the O-anion size [28]. Thus, the observed 'cation size effect' may roughly reflect the change of ionicity in the grain boundary, hence the grain growth behavior. From the viewpoint of the classical ionic radius concept, especially for alkaline earth dopants, a larger substitutional cation should improve the ionicity around the O-anion in the order Mg < Ca < Sr, possibly also suppressing the atomic diffusion in the same order, although this assumption is an oversimplification for transition element dopants.

The microstructural evolution of the GA-M0.5 series at 1,200 °C closely resembled that of the GA-M0.1 series, suggesting that the microstructural evolution generally reflects the effect of the initial dopant segregation process. In the case of GA-M0.5 powders at 1,400 °C, the dopant effect on grain growth was clearly divided into two groups: a retarding group for the Mg, Ca, Sr, Co, Ni, and Zn series and a strong accelerating group for the Cu and Mn series. This accelerating effect on grain growth in GA-Cu0.5 and GA-Mn0.5 samples is in accordance with that reported for CuO [29] and MnO [30] additives to α-alumina powders. Thus, the weakened retarding effect of Cu dopant in GA-Cu0.1 samples suggests that, to some extent, a mechanism similar to that of the GA-Cu0.5 sample, which showed an average grain size of 1.22 μm at 1,400 °C, was at play even at 0.1 mol%. The grain growth in GA-Cu0.5 was presumably accelerated by the formation of a eutectic liquid phase owing to the increased mass transport via a solution-precipitation mechanism [29]. The retarding effect of Mn in the GA-Mn0.1 sample was markedly weakened at 1,400 °C. This also suggests that the mechanism of the accelerating effect, which was exhibited in GA-Mn0.5 samples at 1,400 °C (average grain size: 0.97 μm), started to come out at 0.1 mol%. This accelerating effect of the Mn dopant at high temperatures can be explained in terms of the marked high grain boundary diffusivity reported for

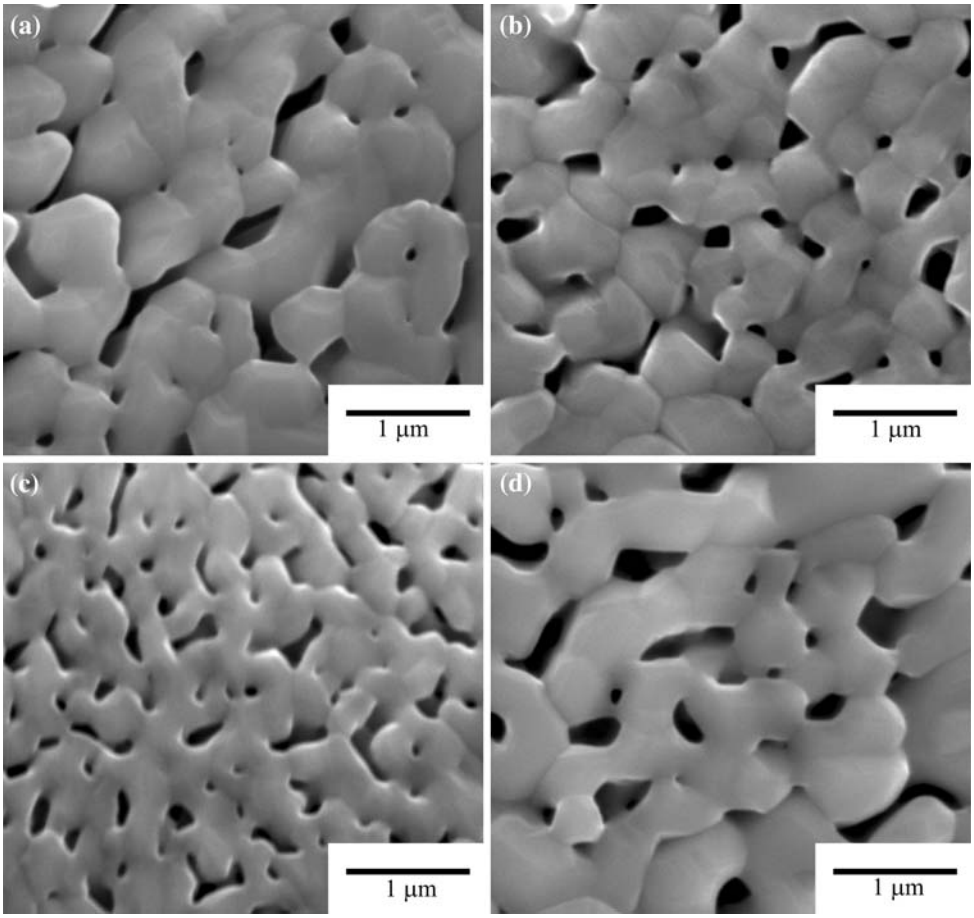

Fig. 8 SEM photographs of typical GA-M01 samples sintered at 1,400 °C for 3 h. (**a**) GA-M0, (**b**) GA-Ni0.1, (**c**) GA-Ca0.1, and (**d**) GA-Cu0.1

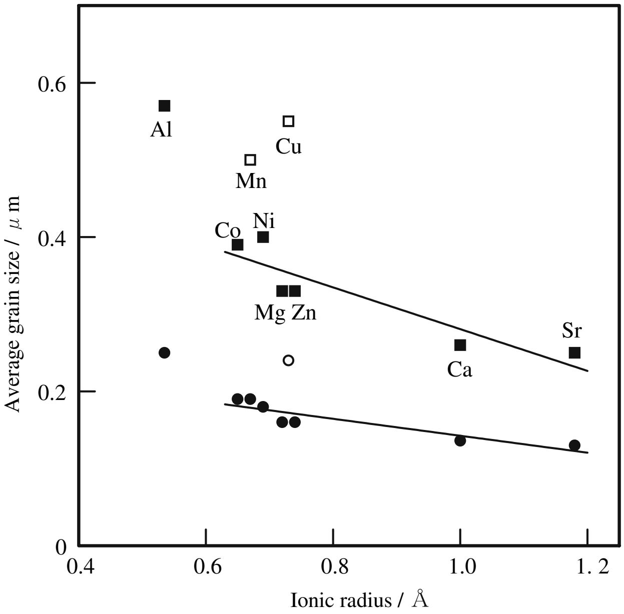

Fig. 9 Average grain size plotted against ionic radius of cation dopant for GA-M0.1 samples sintered at different temperatures. ● and ○: 1,200 °C, ■ and □: 1,400 °C. Open symbols indicate the plots that deviated from the correlation

MnO-doped polycrystalline alumina [28] or the change in the Mn valence as a result of the heating process, which may increase the grain boundary diffusivity [30, 31].

The present results indicate that divalent substitutional dopants below 0.5 mol%, especially a small content of 0.1 mol%, strongly affects the microstructural evolution of GA-M powders at high temperatures, depending on the dopant species. The nanocrystalline nature of GA-M powders also contributes to developing a fine-grained microstructure due to the high dispersion of segregated dopants in the sintering matrices. Thus, the knowledge obtained here extends the potential of the high-purity PHA sol–gel process to the intimate mixing of substitutional dopants at an atomic level and to the fabrication of fine-grained ceramics with the selection of appropriate dopants and sintering conditions. The suppression of the formation of the vermicular microstructure is a problem that needs to be solved for the fabrication of fine-grained alumina ceramics using GA-M powders. The seeding of GA-M powders is a promising way to suppress the formation of the vermicular microstructure [3, 32]. Thus, investigations on the seeding effect on microstructural evolution and densification of GA-M powders are now under way.

Conclusions

M^{2+}-substituted γ-alumina (GA-M; M = Mg, Ca, Sr, Mn, Co, Ni, Cu, and Zn) powders were prepared by a new sol–gel route using high-purity polyhydroxoaluminum (PHA) and MCl_2 solutions, and the effect of substitutional cation dopants ($\leq$ 0.5 mol%) on the phase transformation and microstructural evolution in GA-M powders was systematically investigated. All substitutional divalent dopants examined here retarded the γ-to-α transformation up to 0.3 mol%, depending on the cation dopant content. A correlation was observed between the endothermic DTA peak temperature and the ionic radius of dopant, with the exception of GA-Cu. The microstructural evolution at high temperatures was also strongly affected by dopants that segregated from GA-M primary particles to the grain boundary during/after transformation. Segregation may affect the grain boundary and surface diffusivity in alumina, and hence modulate the grain growth behavior. The dopant effect on grain growth in GA-M powders at 0.1 mol% was all retarding, while that at 0.5% was clearly divided into two groups: a retarding group for the Mg, Ca, Sr, Co, Ni, and Zn series, and an accelerating group for the Cu and Mn series. The average grain size developed at high temperatures seemed to correlate with the dopant ionic radius, except in the case of the Cu and Mn series. The proposed sol–gel route is effective in fabricating fine-grained ceramics through suppressing the formation of a vermicular microstructure.

References

1. Mishra RS, Lesher CE, Mukherjee AK (1996) J Am Ceram Soc 79:2989
2. Kwon O, Nordahl CS, Messing GL (1995) J Am Ceram Soc 78:491
3. Yajima Y, Hida M, Taruta S, Kitajima K (2003) J Ceram Soc Japan 111:110
4. Yajima Y, Hida M, Taruta S, Kitajima K (2003) J Ceram Soc Japan 111:419
5. Yajima Y, Yamaguchi T, Taruta S, Kitajima K (2003) J Ceram Soc Japan 111:786
6. Hida M, Yajima Y, Yamaguchi T, Taruta S, Kitajima K (2006) J Ceram Soc Japan 114:184
7. Coble RL (1961) J Appl Phys 32:793
8. Jorgensen PJ, Westbrook JH (1964) J Am Ceram Soc 47:332
9. Handwerker CA, Morris PA, Coble RL (1989) J Am Ceram Soc 72:130
10. Bae SI, Baik S (1994) J Am Ceram Soc 77:2499
11. Song H, Coble RL (1990) J Am Ceram Soc 73:2077
12. Koyama T, Nishiyama T, Niihara K (1993) J Mater Sci 28:5953
13. C Elsässer G Marinopoulos (2001) Acta Mater 49:2951
14. Hsu Y-F, Wang S-F, Cheng T-W (2003) Mater Sci Eng A362:300
15. Okada K, Hattori A, Taniguchi T, Nukui A, Das RN (2000) J Am Ceram Soc 83:928
16. Saito Y, Takei T, Hayashi S, Yasumori A, Okada K (1998) J Am Ceram Soc 81:2197
17. Ozawa M, Kato O, Suzuki S, Hattori Y, Yamamura M (1996) J Mater Sci Lett 15:564
18. Rossignol S, Kappenstein C (2001) Int J Inorg Mater 3:51
19. Fujita T, Kitajima K, Taruta S, Takusagawa N (1993) Nippon Kagaku Kaishi 319
20. Fujita T, Yamaguchi T, Takusagawa N, Kitajima K (1998) J Ceram Soc Japan 106:1017
21. Mekasuwandumrong O, Praserthdam P, Inoue M, Pavarajarn V, Tanakulrungsank W (2004) J Mater Sci 39:2417
22. Shannon RD (1976) Acta Crystallogr A 32:751
23. Levin I, Brandon D (1998) J Am Ceram Soc 81:1995
24. Lartigue-Korinek S, Legros C, Carry C, Herbst F (2006) J Eur Ceram Soc 26:2219
25. Dynys FW, Halloran JW (1982) J Am Ceram Soc 65:442
26. Wen H-L, Yen F-S (2000) J Cryst Growth 208:696
27. Tartaj J, Zárate J, Tartaj P, Lachowski EE (2002) Adv Eng Mater 4:17
28. Yoshida H, Hashimoto S, Yamamoto T (2005) Acta Mater 53:433
29. Xue LA, Chen I-W (1992) J Mater Sci Lett 11:443
30. Sathiyakumar M, Gnanam FD (2002) Ceram Int 28:195
31. Toy C, Demirci M, Onurlu S, Tasar MS, Baykara T (1995) J Mater Sci 30:4183
32. Kumagai M, Messing GL (1985) J Am Ceram Soc 68:500